Magnetism of one-dimensional Wigner lattices and its impact on charge order

M. Daghofer,[1,2,*] R. M. Noack,[3] and P. Horsch[1]
[1]*Max-Planck-Institut für Festkörperforschung, Heisenbergstrasse 1, D-70569 Stuttgart, Germany*
[2]*Materials Science and Technology Division, Oak Ridge National Laboratory, Oak Ridge, Tennessee 37831, USA and Department of Physics and Astronomy, The University of Tennessee, Knoxville, Tennessee 37996, USA*
[3]*Philipps Universität Marburg, D-35032 Marburg, Germany*
(Received 23 October 2008; published 20 November 2008)

The magnetic phase diagram of the quarter-filled generalized Wigner lattice with nearest-neighbor and next-nearest-neighbor hoppings, t_1 and t_2, is explored. We find a region at negative t_2 with fully saturated ferromagnetic ground states that we attribute to kinetic exchange. Such interaction disfavors antiferromagnetism at $t_2<0$ and stems from virtual excitations across the charge gap of the Wigner lattice, which is much smaller than the Mott-Hubbard gap $\propto U$. Remarkably, we find a strong dependence of the charge structure factor on magnetism even in the limit $U\to\infty$, in contrast to the expectation that charge ordering in the Wigner lattice regime should be well described by spinless fermions. Our results, obtained using the density-matrix renormalization group and exact diagonalization, can be transparently explained by means of an effective low-energy Hamiltonian.

DOI: 10.1103/PhysRevB.78.205115 PACS number(s): 71.10.Fd, 71.45.Lr, 73.20.Qt, 75.30.Et

I. INTRODUCTION

In a Wigner lattice (WL), long-range Coulomb repulsion dominates over the kinetic energy of electrons and leads to strong and well-defined charge order.[1] Originally introduced for the electron gas with a homogeneous neutralizing background, this concept was generalized to electrons on a lattice by Hubbard.[2] Evidence for quasi-one-dimensional (1D) Wigner lattices has been found in organic[3–6] and anorganic[7–10] chain compounds, nanowires,[11] and in carbon nanotubes.[12] Low-dimensional WLs are favored by reduced screening.[2,13] Moreover, strong correlations induced by large local Hubbard interaction U suppress screening further and protect the long-range nature of the Coulomb repulsion.[10] It is, however, not straightforward to distinguish a true WL from a quantum-mechanical charge-density wave (CDW) simply on the basis of the periodicity of the charge modulation. In fact, it turns out that the modulation period of the WL coincides with that of the $4k_F$ CDW.[2,4,14–16] This may be surprising as the microscopic origin of the charge order in the two cases is fundamentally different.[6] (i) The mechanism for the WL is based solely on the classical Coulomb repulsion and is dependent only on the charge of electrons and not on their fermionic nature. The periodicity follows simply from the configuration of charges with minimal energy. (ii) Instead, the quantum-mechanical CDW depends on the Fermi-surface topology and the instability and modulation reflects the Fermi momentum k_F.

If we allow for nearest-neighbor (NN) and next-nearest-neighbor (NNN) hoppings, t_1 and t_2, we arrive at an even more interesting model which, depending on the relative size and sign of t_1 and t_2, may have an electron dispersion with two minima instead of one.[17,18] Actually, it has been proposed that the edge-sharing CuO chain compounds are described by such models with $|t_2|>|t_1|$.[10] It is then immediately obvious that in the case of a four-Fermi-point topology the periodicities of WL and CDW no longer coincide. We note that the experimentally observed charge modulations in the edge-sharing compounds $Na_{1+x}CuO_2$ (Refs. 10 and 19–21) are strong and their periodicity consistent only with that of the WL. Another possible type of instability in the presence of strong correlations, namely, the $2k_F$ Peierls and spin-Peierls modulations,[16,22] which requires a distortion of the lattice, appears to be ruled out in these systems. Doped edge-sharing chains are also the building blocks of the $Ca_{2+x}Y_{2-x}Cu_5O_{10}$ (Refs. 9 and 23) and the $Sr_{14-x}Ca_xCu_{24}O_{41}$ (Refs. 7, 8, and 24) systems, and pronounced charge order has been observed in these compounds as well.

Here we shall investigate the intrinsic mechanisms for the magnetism of generalized Wigner lattices. It is well known that NNN hopping t_2 has nontrivial consequences for magnetism in the 1D Hubbard model at general filling and may lead to ferromagnetic (FM) states in certain cases.[25–29] It should be kept in mind that, according to the Lieb-Mattis theorem,[30] ferromagnetism is excluded at any filling in the 1D Hubbard model with NN hopping (i.e., $t_2=0$). For the 1D Hubbard model with NN and NNN hoppings, Pieri *et al.*[27] and Daul and Noack[28] found that ferromagnetic ground states appeared above a critical U in those regions of the t_1-t_2 plane where four Fermi points exist. These results were obtained in the metallic regime where the relevance of Fermi-surface topology is suggestive; however, the implications for the localized electrons of a Wigner crystal are unclear.

The magnetism of generalized WLs is typically discussed in terms of effective Heisenberg models where the position of the spins is dictated by the charge order pattern of the WL.[10,31,32] The prevailing superexchange interactions are antiferromagnetic. However, there are also ferromagnetic couplings in edge-sharing chains due to the Hund interaction at the oxygen ligands that may be larger than the AF interactions and render, e.g., the nearest-neighbor interaction J_1 ferromagnetic.[10,33,34] These features lead to frustration, and the resulting helical spin states have been observed in the spin-1/2 edge-sharing chain compounds $LiCu_2O_2$ (Ref. 35) and $NaCu_2O_2$.[36–38]

In this paper, we show that for a Wigner crystal at quarter filling, there is another intrinsic mechanism that may lead to

ferromagnetism. By means of a density-matrix renormalization-group (DMRG) study of the t_1-t_2 Hubbard-Wigner model, which includes local Hubbard U and long-range Coulomb interactions $V_l=V/l$, we show that there is a regime of fully polarized FM states at negative t_2. Subsequently, we derive an effective magnetic Hamiltonian for the Wigner-lattice regime, i.e., $|t_1|,|t_2| \ll V < U$, and show that the emergence of ferromagnetism can be explained by an effective *kinetic exchange* mechanism mediated by NNN hopping t_2. The associated magnetic exchange constant $\propto t_1^2 t_2/\epsilon_0^2$ depends on the sign of t_2 and therefore kinetic exchange is found to favor ferromagnetism for negative t_2 and antiferromagnetism for positive t_2. Kinetic exchange involves excitations across the charge gap ϵ_0 of the WL but not across the usually much larger Mott-Hubbard gap $\sim U$, as is the case for AF superexchange or for many realizations of FM three-particle ring exchange.[39] The charge gap ϵ_0 of the generalized WL depends sensitively on the commensurability with the underlying crystalline lattice. At quarter filling this gap is particularly large $\epsilon_0 \sim V/2$.

If the charge gap $\epsilon_0 \sim V/2$ of the WL is much larger than the hopping amplitudes, t_1 and t_2, and any expected magnetic couplings, a separation of charge and magnetic energy scales appears straightforward. Hence, charge ordering in a WL is usually discussed in terms of spinless fermions. Magnetism, e.g., antiferromagnetic (AF) superexchange or FM Hund's rule[10] and three-site ring exchange,[40] is then treated as a perturbation given a particular charge-ordering pattern. One would, however, not expect the magnetic order to have a strong impact on the underlying charge order because the magnetic energy scale is so much smaller than the dominant Coulomb repulsion for all these processes.[41] The motivation for this work was the initial observation that the charge structure of the WL measured by the charge structure factor $N(q)$ at $q=\pi$ is strongly affected by electron spin, in disagreement with the calculation for spinless fermions. Yet there is a region in the t_1-t_2 phase diagram at negative t_2 where $N(\pi)$ is the same for spinless fermions and for fermions with spin. Moreover, $N(\pi)$ does not depend on t_2 in that parameter range. The obvious conjecture is that the ground state should be fully spin polarized in this regime.

We show here that due to the kinetic exchange mechanism, these FM ground states emerge and that the kinetic exchange processes have a surprisingly strong impact on the charge ordering in spite of the classical origin of the WL. Indeed, the AF state at $t_2>0$ has dramatically weaker charge order than the ferromagnetic or spinless states. While the charge order is reduced $\propto t_2$ for positive t_2, it does not depend on t_2 in the FM regime $t_2^a > t_2 > t_2^b$ with negative t_2. Remarkably, for negative t_2 values below t_2^b, AF reappears; yet the charge order then increases with increasing modulus $|t_2|$. The boundaries of the FM phase follow from the effective spin Hamiltonian as $t_2^a \sim -3t_1^2/U$ and $t_2^b \sim -(U/\epsilon_0^2)t_1^2$ and match the magnetic phase boundaries found using the DMRG. This peculiar behavior is due to a purely quantum effect involving destructive interference of kinetic exchange processes in the FM state due to the Pauli principle and constructive interference for the AF case.

The paper is organized as follows. After introducing the Hubbard-Wigner Hamiltonian in Sec. II, we present results for the charge structure factor for spinless fermions interacting via long-range Coulomb interaction in Sec. III. We shall see that the results for spinless fermions coincide with results for electrons with spin in some region of the t_1-t_2 phase diagram, while they are substantially different in other parts of the phase diagram. We derive an effective Heisenberg Hamiltonian in Sec. IV and show that the magnetic phase diagram, i.e., the appearance of the fully saturated FM phase and its phase boundaries, can be naturally explained. Next we show that the peculiarities found numerically for the charge structure factor find a straightforward analytical description in the framework of the effective Hamiltonian. Finally, we discuss and summarize our results in Sec. V.

II. HUBBARD-WIGNER MODEL

The Hubbard-Wigner Hamiltonian investigated in this paper is motivated by the one-dimensional edge-sharing CuO-chains.[10,42] Edge-sharing chains are formed by CuO_4 squares just as in the CuO planes of the high-T_c compounds; but these units are differently linked. The edge-sharing arrangement leads to small nearest-neighbor hopping matrix element t_1 due to the almost 90° Cu-O-Cu coordination and some contribution to t_1 stems from direct Cu d-d overlap.[43] Moreover, the structure leads to a comparatively large matrix element t_2 between second-neighbor Cu ions stemming from a Cu-O-O-Cu path.[33] Thus edge-sharing chains, in contrast to the 180° bonded high-T_c cuprates, fulfill the fundamental criterion for a WL, namely, that the kinetic energy is small compared to the nearest-neighbor Coulomb interaction, in an optimal way. While the Coulomb repulsion is screened by a static dielectric constant in these insulators, the one over distance decay of the interaction is preserved and must be taken into account. Truncation of the interaction may have serious consequences for the charge-order pattern of generalized WLs (Ref. 2) as well as for their charge excitations.[42,44]

The relevant states of Cu that need to be included in a low-energy model are: Cu^{3+} or, more precisely, the Cu d^9-ligand hole singlet state, Cu^{2+} with spin-1/2, and Cu^{1+} corresponding to the filled d shell. These states can be expressed in the frame of a single-orbital Hubbard model with 0, 1, or 2 electrons per site. Thus we consider the Hubbard-Wigner Hamiltonian where the extension Wigner indicates that the long-range Coulomb interaction is included. This model has the form,[10,42]

$$H = -t_1 \sum_{i,\sigma} (c^\dagger_{i,\sigma} c_{i+1,\sigma} + \text{H.c.}) - t_2 \sum_{i,\sigma} (c^\dagger_{i,\sigma} c_{i+2,\sigma} + \text{H.c.}) + U \sum_i n_{i,\uparrow} n_{i,\downarrow} + \sum_{l=1}^{L/2} V_l \sum_i (n_i - \bar{n})(n_{i+l} - \bar{n}), \quad (1)$$

where the operators $c^\dagger_{i,\sigma}$ $(c_{i,\sigma})$ create (destroy) electrons with spin σ at lattice site i, with $i=1 \ldots L$. The local density is given by $n_{i,\sigma}=c^\dagger_{i,\sigma} c_{i,\sigma}$ and $n_i=n_{i,\uparrow}+n_{i,\downarrow}$ and the average density is $\bar{n}=N_e/L$ for N_e electrons. The kinetic-energy term includes NN hopping t_1 and NNN hopping t_2, which are both typically much smaller than either the on-site Coulomb repulsion U or the NN-Coulomb interaction V that parametrizes the long-range Coulomb interaction $V_l=V/l$. In the

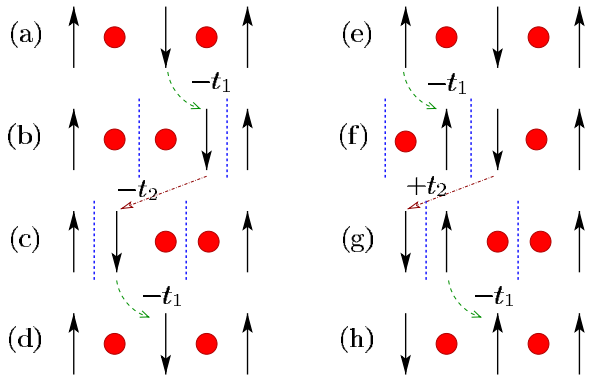

FIG. 1. (Color online) Schematic depiction of relevant $\propto t_1^2 t_2/\epsilon_0^2$ kinetic exchange processes. We start from perfect charge order (a) and (e), where circles denote empty sites (Cu^{3+} atoms in $Na_{1+x}CuO_2$), and arrows denote occupied sites (Cu^{2+}). NN hopping t_1 induces excitations (a→b and e→f) with two domain walls (dashed lines) and cost ϵ_0. Two different t_2 processes, one with (f→g) and one without (b→c) electron exchange, become possible. For FM spins (triplet channel) or spinless fermions, however, these two processes (a→d) and (e→h) cancel exactly because of the relative Fermi sign in the next-nearest-neighbor hopping process.

case of finite rings of length L, we truncate the $1/l$ behavior at $L/2$, which is equivalent to replacing V/l by $\max[V/l, V/(L-l)]$ for $0<l<L$. We have verified that small modifications to the $1/l$ behavior do not affect our results. In fact, truly long-range Coulomb repulsion is not crucial for the results presented here. At quarter filling, both the FM kinetic exchange and the weakened charge order can also be seen for on-site U and NN Coulomb repulsion V_1 only. In the following, we consider the model with long-range Coulomb interaction and use the NN Coulomb repulsion $V_1=V$ as unit of energy. Without loss of generality, t_1 is chosen to be positive. The Hamiltonian in Eq. (1) contains two ingredients that have been shown to favor FM correlations in Hubbard-type models: Strong on-site and longer-range Coulomb repulsion[45] and, perhaps more importantly, NNN hopping.[26–28,46] In this paper we address the most transparent instance of the WL, namely, quarter filling $\bar{n}=0.5$ for Hamiltonian (1). We explore the magnetic properties within the WL regime, i.e., $t_1, |t_2| \ll V \ll U$, which have not been explored before, and find FM ground states in a region of the t_1-t_2 phase diagram with negative t_2. Quite unexpectedly, we also find a strong influence of magnetism on WL charge order. For comparison, we will first discuss the charge ordering for spinless fermions at half filling, corresponding to the fully spin-polarized case with $\bar{n}=0.5$. At small t_1 and t_2, the alternating charge order is very rigid and its lowest charge excitations are domain walls (DWs) with fractional charge.[2,47,48] DWs can be induced in a perfectly ordered state via NN hopping t_1, as schematically illustrated in Fig. 1. Their creation costs energy of $\epsilon_0 \sim V/2$ in the case of long-range Coulomb interaction, and once created they can move easily through the lattice via t_1 hopping processes. Their fractional charge $\pm 1/2$ is responsible for the distinctive WL features in the optical conductivity and in photoemission.[42,44,49]

We investigate this model with exact diagonalization (ED) for spinless Fermions and chains of up to $L=28$ sites. We use

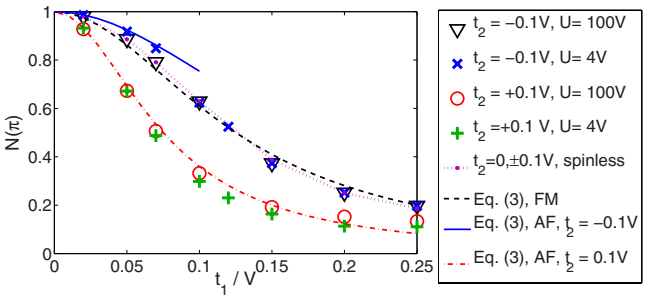

FIG. 2. (Color online) Charge structure factor $N(q)$ for $q=\pi$ as a function of nearest-neighbor hopping t_1. The dotted line for spinless fermions is from ED calculations with $L=28$; symbols were calculated using the DMRG with $L=24$ for electrons with spin. Analytic results are obtained from Eq. (4) with $\Delta=\epsilon_0$ (FM) and $\Delta=\epsilon_0-2t_2$ (AF), respectively.

the Lanczos algorithm with a numerical accuracy of $\approx 10^{-6}$ and check its validity by use of full diagonalization for up to 18 sites. These ED calculations were done for both the ground state ($T=0$) and for small but finite temperatures ($T=10^{-4}-10^{-3}$) leading to practically identical results at small t_1 and t_2 because there is a finite charge gap of $\epsilon_0 \approx V/2$, which blocks changes at temperatures with an energy scale smaller than this. For electrons with spin, we use the DMRG with chains of $L=24,32,40$ and find results consistent with the ED for spinless fermions. In the DMRG, we keep 200–1200 states at each step, performing up to 10 finite-size sweeps, and the neglected weight is $\lesssim 10^{-5}$. For parameters with a FM ground state, the energy obtained with the DMRG agrees with the ED result.

III. CHARGE ORDER

Increasing the NN hopping t_1 gradually reduces the charge ordering[42] until, at $t_1 \sim 0.2$ V, the charge gap vanishes.[13] This is reflected in the charge structure factor,

$$N(q) = \langle \rho_{-q} \rho_q \rangle, \quad \text{with} \quad \rho_q = 1/N_e \sum_r \exp(-iqr) n_r, \quad (2)$$

which, for perfect charge alternation, is peaked at $q=\pi$ with $N(\pi)=1$. As can be seen in Fig. 2, the results for spinless fermions, obtained using Lanczos diagonalization, show that $N(\pi)$ is strongly reduced even before the gap vanishes, giving a weaker charge-density wave. We find that, for spinless fermions, the melting of WL charge order with t_1 does *not* depend on t_2. The behavior of $N(\pi)$ can be described analytically because only few DWs are present at small t_1. To leading order, virtual DW excitations contribute

$$E_c \sim -N_e 2t_1^2/\epsilon_0 \quad (3)$$

to the ground state energy. With $N_e=L/2$, we obtain

$$N(\pi) \simeq \frac{1}{1+(4t_1/\Delta)^2}, \quad (4)$$

given the charge gap $\Delta=\epsilon_0 \sim V/2$. This expression is indicated by the dashed line in Fig. 2 and agrees with the numerical data.

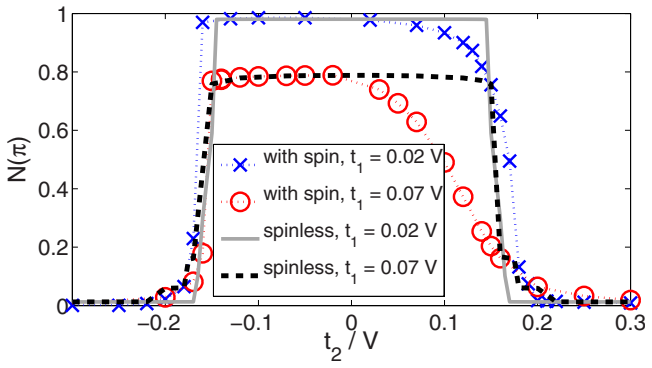

FIG. 3. (Color online) The charge structure factor $N(\pi)$ versus t_2. Note that it does depend on the sign of t_2 for fermions with spin and does not for spinless fermions. The results for spinless fermions were calculated using exact diagonalization ($L=18$) and the results for electrons with spin using the DMRG ($t_1=0.02$ V, $U=4$ V, and $L=24$; $t_1=0.07$ V, $U=100$ V, and $L=32$).

In marked contrast to the gradual change that occurs with t_1, NNN hopping t_2 is frustrated for spinless fermions until $N(\pi)$ drops sharply at a level-crossing transition at $t_2^c \sim 0.15$ V (Ref. 42) (see also Fig. 3). At the level crossing, the ground state changes fundamentally; $N(q)$ develops a broad continuum with a maximum between π and $\pi/2$ (moving to $\pi/2$ at large t_2) rather than at π. Just as t_2 does not influence how charge order weakens with t_1, the level-crossing transition driven by t_2 is hardly affected by t_1. This can be seen by comparing the $t_1=0.02$ and 0.07 V curves for spinless fermions in Fig. 3. Consequently, the WL phase is bounded by vertical and horizontal lines in the t_1-t_2 plane (see Fig. 4).

While the transition between the two CDW phases with $q=\pi$ and $q\neq\pi$ depends on both t_1 and t_2, it is remarkable that the WL is never affected by the *combination* of hopping processes. We would actually expect some cooperative effects between t_1 and t_2 because NNN hopping is no longer

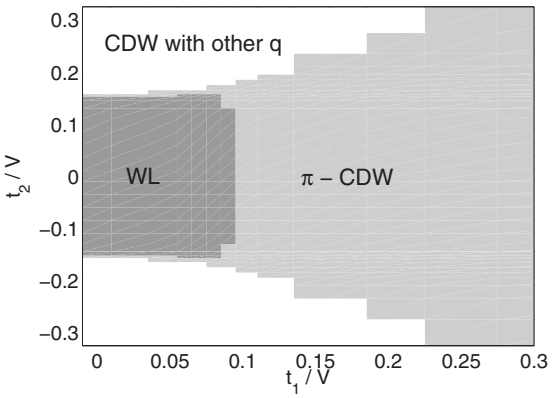

FIG. 4. Phase diagram for spinless fermions determined from the charge structure factor $N(q)$ [see Eq. (2)]. WL (dark gray): strongly charge-ordered WL with $N(\pi)>0.7$. π-CDW (light gray): CDW with periodicity π but $N(\pi)<0.7$. (This choice corresponds approximately to the inflection point of $N(\pi)$ as a function of t_1.) In the white area, $N(q)$ has its maximum at $\pi/2\leq q<\pi$, at $\pi/2$ for large t_2. In the exact diagonalization, we take $N_e=8$ fermions on $L=16$ sites.

frustrated in the presence of t_1 (see Fig. 1). Due to the DW delocalization, (b$\leftrightarrow$c), two-DW states should gain energy with t_2, and nonzero t_2 should thus help destabilize the charge ordering. The solution is found in the process shown in (f$\leftrightarrow$g): For spinless fermions (all arrows in Fig. 1 pointing up), process (a$\leftrightarrow$e) and process (f$\leftrightarrow$g) are equivalent. Since two electrons swap places in the second case, the resulting Fermi sign leads to destructive interference and the lowest-order processes associated both with t_1 and with t_2 cancel out.

After this discussion of the spinless model, we now turn to electrons with spin. Due to the dominance of the Coulomb repulsion and the classical nature of WL ordering, we might not expect charge ordering to be affected significantly by the spin degree of freedom as long as $U\gg V$. However, the behavior of $N(\pi)$ obtained using the DMRG for electrons with spin indicates that there is a surprisingly strong influence even for $U=100$ V. In contrast to spinless fermions, where t_2 does not affect the behavior of $N(\pi)$ as a function of t_1, we find the charge order to be considerably weakened at $t_2>0$ for electrons with spin (see Fig. 2). We can understand this by considering the processes of Fig. 1. The states depicted in (c) and (g) differ by their sequence of up and down spins. Process (b$\leftrightarrow$c) is then no longer canceled by (f$\leftrightarrow$g), as it is for spinless fermions. Consequently, a kinetic-energy contribution $\propto t_1^2 t_2/\epsilon_0^2$ is no longer forbidden by the Pauli principle.

Our interpretation is corroborated by analytic considerations. The additional DW motion due to t_2 favors two-DW states and changes the gap relevant to Eq. (4) from $\Delta=\epsilon_0 \sim V/2$ to $\Delta=\epsilon_0-2t_2$. This leads to the dash-dotted line in Fig. 2, which indeed describes the weakened charge order seen in the DMRG at $t_2>0$. For $t_2<0$, however, the DMRG results are described by the *spinless* gap $\Delta=\epsilon_0$. Since spinless fermions are equivalent to the fully polarized FM state, this indicates *ferromagnetism*, see below. For $U=4$ V and small $t_1\lesssim 0.07$ V, where AF superexchange $\sim 4t_2^2/U$ destroys the polarized state, processes $\propto t_1^2 t_2$ retain their impact and *strengthen* charge order, see the full line in Fig. 2.

For fermions with spin, the sharp transition as a function of t_2 shown in Fig. 3 becomes asymmetric with respect to the sign of t_2. Even for very small $t_1=0.02$ V, the cooperation between t_1 and t_2 is enough to render the breakdown of the WL charge order more gradual for $t_2>0$ than for $t_2<0$. For $t_1=0.07$ V, charge order is strongly reduced for $t_2>0$, and the sharp drop in $N(\pi)$ as a function of t_2 has disappeared, in stark contrast to the spinless model.

IV. MAGNETISM

One expects AF interactions for the WL (Ref. 41) due to superexchange in the generalized Hubbard model. Yet our observation that the charge structure factor at negative t_2 agrees closely with results for spinless fermions (see Figs. 2 and 3) is already an indication that the ground state in this regime is FM. This is indeed the case, and our DMRG studies in fact yield fully polarized ground states for some parameter sets at negative t_2. As can be seen in Fig. 5, the FM interval increases with t_1.

In the following, we analyze the magnetic exchange by using perturbation theory valid when $t_1, t_2 \ll V \ll U$. The ro-

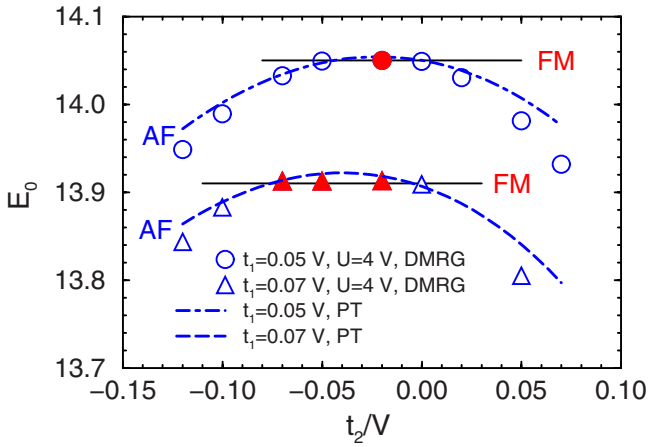

FIG. 5. (Color online) Ground-state energy E_0 for $L=24$ versus t_2 for $U=4$ V with $t_1=0.05$ V (circles) and $t_1=0.07$ V (triangles). Filled symbols indicate a fully polarize ground state and horizontal lines the energy of the FM state at $t_2=0$. The dashed and dash-dotted lines are analytic results obtained from perturbation theory [Eq. (8)] see text.

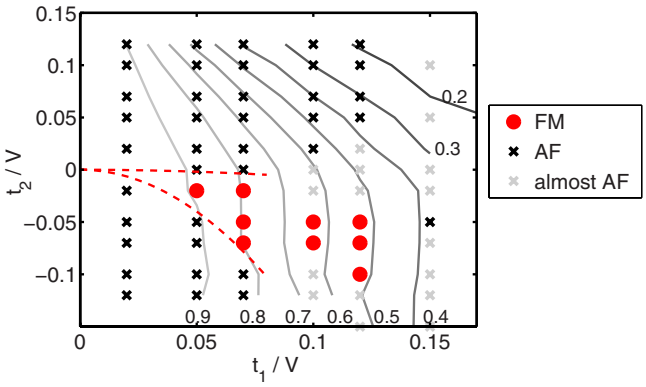

FIG. 6. (Color online) Magnetic phases and charge structure in the WL regime. FM (°): $m>0.99M$; AF (black ×): $m<0.01M$; "almost AF" (gray ×): $0.01M\leq m<0.1M$, where $m=S_{\rm tot}(S_{\rm tot}+1)$ was obtained by DMRG for $L=24$, $U=4$ V, and $M=S_{\rm max}(S_{\rm max}+1)=42$. Gray lines give potential lines for $N(\pi)$, i.e., the strength of the alternating charge order. The lines were interpolated from data points obtained at the same parameter values as the magnetic data.

bust WL charge order leads to a *modulated* Heisenberg chain with spins at every second lattice site. Magnetism is therefore described by an effective Heisenberg-type Hamiltonian,

$$H_J = J\sum_i \left(\mathbf{S}_i\cdot\mathbf{S}_{i+2} - \frac{1}{4}n_i n_{i+2}\right), \tag{5}$$

where i runs only over the even sites, where the $L/2$ spins forming the WL are located. The total ground-state energy then is $E=\langle H_J\rangle+E_{\rm FM}$, where $E_{\rm FM}$ is the energy of the fully spin-polarized state, which is equivalent to the ground-state energy of spinless fermions. There are two distinct mechanisms that contribute to the exchange constant $J=J_{\rm SE}+J_{\rm KE}$. The first term is the usual superexchange, which involves a doubly occupied intermediate state and therefore has the energy scale U in the denominator,

$$J_{\rm SE} \simeq \frac{4t_2^2}{U} + \frac{12t_1^4}{\epsilon_0^2 U} + \frac{8t_1^2 t_2}{\epsilon_0 U} + \ldots \tag{6}$$

The second term $J_{\rm KE}$—denoted as the *kinetic exchange*—arises from a spin exchange without any doubly occupied sites, i.e., exactly from the same effect that weakens the charge order for $t_2>0$. Quantum interference between processes (a↔e) and (f↔g) in Fig. 1 is *destructive* in the polarized FM state and *constructive* in the AF singlet, which leads to an exchange energy,

$$J_{\rm KE} \simeq \frac{2t_1^2}{\epsilon_0}\left(\frac{1}{1-2t_2/\epsilon_0}-1\right) \simeq \frac{4t_1^2 t_2}{\epsilon_0^2} + \ldots \tag{7}$$

that depends on the sign of t_2. The NN correlation function of the 1D quantum antiferromagnet is given by $\kappa=-\ln 2+1/4\approx -0.443$, corresponding to $\langle\mathbf{S}_i\cdot\mathbf{S}_{i+2}\rangle$ for our modulated chain. Inserting κ as well as Eqs. (6) and (7) into Eq. (5), we obtain an analytic estimate, valid at small hopping, for the energy of the AF state,

$$E_{\rm AF} \simeq \frac{L}{2}(J_{\rm SE}+J_{\rm KE})(\kappa-1/4)+E_{\rm FM}. \tag{8}$$

We compare this analytic result to numerical DMRG data for $t_1=0.05$ V and 0.07 V, in Fig. 5. This figure shows that the analytic curves given by $E_0=\min(E_{\rm AF},E_{\rm FM})$ closely model the numerical ground-state energies for not-too-large t_2 with no fitting parameters. Moreover, the analytical boundaries of the FM phase, namely, $t_2^a\sim -3t_1^2/U$ and $t_2^b\sim -(U/\epsilon_0^2)t_1^2$, match the magnetic phase boundaries found using the DMRG.

This may be compared with the boundaries in the t_1-t_2 plane describing the appearance of four Fermi points, namely, $t_2\leq -(t_1/4)\sec(\pi n/4)^2$ and $t_2\geq(t_1/4)\csc(\pi n/4)^2$, where n is the filling. For the quarter-filled case, i.e., $n=1/2$, only the first relation is of interest and yields the condition $-\infty\leq t_2\leq -0.293t_1$ for the appearance of FM in the Hubbard model, as observed in Refs. 27 and 28. It is perhaps not surprising that the boundary relevant for the Hubbard model, which is linear in t_1, is completely different from the boundaries obtained for the Wigner lattice, which are both quadratic in t_1. Nevertheless, ferromagnetism at quarter filling is found at negative t_2 in both cases.

The phase diagram in Fig. 6 shows the total spin in the ground state of a chain with $L=24$ for the range of t_1,t_2 corresponding to the WL regime. The dashed lines represent the analytical boundaries, t_2^a and t_2^b, of the FM region. Kinetic exchange Eq. (7)—the only magnetic interaction surviving for $U\to\infty$—is AF for $t_2>0$. For $t_2<0$, $J_{\rm KE}$ raises the energy of the AF state over that of the FM state (see Fig. 5). In the FM state itself, this effective FM exchange is, ironically, *absent* because the Pauli principle forbids the ring exchange in the polarized state. At large negative t_2 and not-too-large U, AF superexchange (6) once again dominates.

The phase diagram Fig. 6 also contains contour lines $N(q=\pi,t_1,t_2)=C$, with the constant $C=0.9,0.8,\ldots,0.4$, which indicate the strength of the alternating $(q=\pi)$ charge order of the Wigner lattice. In accordance with Figs. 2 and 3,

we find that the charge order dies off most quickly in the singlet states in the $t_2>0$ region. The analytic contour lines t_1^c versus t_2 following from Eq. (4) for $t_2>0$ have the form,

$$t_1^c \simeq \frac{1}{4}(\epsilon_0 - 2t_2)\sqrt{1/N(\pi) - 1}. \quad (9)$$

They agree with the DMRG data, just as Eq. (4) agrees with $N(\pi)$ in Fig. 2. Since our analytic result describes the unbiased DMRG simulations so well, we conclude that the kinetic exchange indeed drives the suppression of charge order in the AF regime for $t_2>0$.

V. DISCUSSION AND CONCLUSIONS

We have investigated charge order and magnetism of the 1D quarter-filled Wigner lattice with nearest-neighbor and next-nearest-neighbor hoppings. Starting from the regime $t_1, |t_2| \ll V$ with extremely strong alternating charge order stabilized by the long-range Coulomb repulsion, we find that increasing NN hopping t_1 drives a crossover to a $4k_F$ charge-density state with weaker charge order but unchanged modulation period, whereas increasing NNN hopping t_2 leads to a sudden level-crossing transition, destroying the alternating charge order.[42] For $t_1, |t_2| \ll V$ and spinless fermions, we find that there are no mixed processes involving both t_1 and t_2 because destructive interference removes the lowest-order processes $\propto t_1^2 t_2$. Consequently, the WL is bounded by a vertical crossover line and horizontal phase transition lines in the t_1-t_2 phase diagram for spinless fermions (see Fig. 4).

However, in the case of real electrons with spin, we find that processes $\propto t_1^2 t_2$ are absent in the FM state (as for spinless fermions) but not in the AF state (as illustrated in Fig. 1). This results in an effective magnetic exchange $\simeq 4t_1^2 t_2/\epsilon_0^2$ which favors the AF relative to the FM state for positive t_2 and disfavors the AF state for negative t_2. This peculiar effect is corroborated by DMRG data, where we indeed find AF as well as FM ground states which depend on t_1 and t_2. The phase boundaries of the FM phase obtained here for the quarter-filled WL are distinct from those obtained for the t_1-t_2 Hubbard models driven by large U and Fermi-surface topology, where ferromagnetism is found whenever the fully polarized Fermi sea is split in two.[27] This is perhaps not that surprising, as the charge order in the WL is not caused by a quantum mechanical Fermi-surface instability but by the strong Coulomb repulsion, which does not depend on the Fermi surface. Thus, the situation in the WL is very different from charge and magnetic order driven by Fermi-surface instabilities in the Hubbard model with purely on-site Coulomb repulsion, which was studied extensively in Ref. 16.

Magnetism in the WL is not driven by Fermi-surface instabilities but actually has more in common with the FM reported for a model of coupled chains with a symmetry-breaking on-site potential.[26] In these coupled chains, charge order is stabilized by a strong on-site potential, which corresponds to the spontaneous symmetry breaking by long-range Coulomb repulsion in the case of the WL and is likewise independent of the Fermi surface. Starting from strong charge order, we have been able to derive the effective magnetic exchange terms using perturbation theory and find the resulting magnetic energy to be in good agreement with DMRG data (see Fig. 5). The most important terms in the effective exchange Hamiltonian are the AF superexchange $\propto t_2^2/U$ involving a doubly occupied site and the *kinetic* exchange term $\propto t_1^2 t_2/V^2$. A related FM exchange mechanism based on strong charge ordering and NN hopping has been invoked for two-dimensional kagome lattices.[50]

Since neither charge order nor magnetism are driven by a Fermi-surface instability but are determined by the Coulomb interactions, one might not expect that the charge order depends significantly on the magnetic correlations. Indeed, Wigner lattices are often discussed in terms of spinless fermions, and the magnetic exchange is added only in terms of a modulated Heisenberg model for the given charge order. Our calculations show that this picture is too simple. Figures 2 and 3 reveal that magnetic correlations have a very strong impact indeed on charge order. In fact, the weakening of charge order in the AF phase at positive t_2 is due to the same processes $\propto t_1^2 t_2$ that cause the kinetic exchange. While these virtual processes cancel in the FM phase, they involve domain-wall excitations in the AF phase, see the sketch in Fig. 1. Controlled by the t_2 dependent two-DW gap Δ, the admixture of virtual DW excitations leads to a reduction in charge order in the AF state at positive t_2, as can be seen in the phase diagram Fig. 6. Within the FM regime at negative t_2, charge order does not depend on t_2. At large negative t_2, however, the antiferromagnetic phase reappears, but now, surprisingly, the charge order becomes stiffer as $|t_2|$ is increased. This peculiar behavior finds its explanation in the t_2 dependence of the domain-wall gap Δ in the AF state.

In summary, we have shown that in Wigner lattices with next-nearest-neighbor hopping t_2, a *kinetic exchange mechanism* is at work, which favors ferromagnetism for negative NNN hopping t_2 and might explain the spin polarization recently observed in strongly charge-ordered carbon nanotubes.[12] In contrast to the usual superexchange processes, which involve virtual excitations across the Mott-Hubbard gap $\sim U$, kinetic exchange arises from virtual transitions across the Wigner lattice charge gap $\epsilon_0 \propto V \ll U$. Although Fermi-surface topology describes neither charge nor magnetic order in the strongly correlated WL, we nevertheless find that quantum interference of electrons is important in the WL. In fact, the spin degrees of freedoms have such a strong impact in the AF regime that charge ordering *cannot* be described reliably in terms of spinless fermions even in the extreme WL regime $t_1, |t_2| \ll V \ll U$. As this effect is intimately related to the kinetic exchange mechanism, it may also be relevant in higher dimensions, e.g., the above-mentioned kagome systems.

ACKNOWLEDGMENTS

We thank D. Baeriswyl, K. Hallberg, M. Jansen, N. Kawakami, B. Keimer, G. Khaliullin, S. Maekawa, W. Metzner, C. Penc, R. Zeyher, and T. Tohyama for useful discussions. This research (M.D.) was partly supported by the NSF under Grant No. DMR-0706020.

*m.daghofer@fkf.mpg.de

[1] E. Wigner, Phys. Rev. **46**, 1002 (1934).
[2] J. Hubbard, Phys. Rev. B **17**, 494 (1978).
[3] K. Hiraki and K. Kanoda, Phys. Rev. Lett. **80**, 4737 (1998).
[4] F. Nad and P. Monceau, J. Phys. Soc. Jpn. **75**, 051005 (2006).
[5] R. T. Clay, R. P. Hardikar, and S. Mazumdar, Phys. Rev. B **76**, 205118 (2007).
[6] T. Kakiuchi, Y. Wakabayashi, H. Sawa, T. Itou, and K. Kanoda, Phys. Rev. Lett. **98**, 066402 (2007).
[7] D. E. Cox, T. Iglesias, K. Hirota, G. Shirane, M. Matsuda, N. Motoyama, H. Eisaki, and S. Uchida, Phys. Rev. B **57**, 10750 (1998).
[8] M. Matsuda, T. Yosihama, K. Kakurai, and G. Shirane, Phys. Rev. B **59**, 1060 (1999).
[9] K. Kudo, S. Kurogi, Y. Koike, T. Nishizaki, and N. Kobayashi, Phys. Rev. B **71**, 104413 (2005).
[10] P. Horsch, M. Sofin, M. Mayr, and M. Jansen, Phys. Rev. Lett. **94**, 076403 (2005).
[11] A. Rahman and M. K. Sanyal, Phys. Rev. B **76**, 045110 (2007).
[12] V. V. Deshpande and M. Bockrath, Nat. Phys. **4**, 314 (2008).
[13] S. Capponi, D. Poilblanc, and T. Giamarchi, Phys. Rev. B **61**, 13410 (2000).
[14] J. E. Hirsch and D. J. Scalapino, Phys. Rev. Lett. **50**, 1168 (1983).
[15] H. J. Schulz, Phys. Rev. Lett. **71**, 1864 (1993).
[16] C. Schuster and U. Schwingenschlögl, Phys. Rev. B **75**, 045124 (2007).
[17] M. Fabrizio, Phys. Rev. B **54**, 10054 (1996).
[18] R. Arita, K. Kuroki, H. Aoki, and M. Fabrizio, Phys. Rev. B **57**, 10324 (1998).
[19] M. Sofin, E.-M. Peters, and M. Jansen, J. Solid State Chem. **178**, 3708 (2005).
[20] S. van Smaalen, R. Dinnebier, M. Sofin, and M. Jansen, Acta Crystallogr., Sect. B: Struct. Sci. **63**, 17 (2007).
[21] M. Raichle, M. Reehuis, G. André, L. Capogna, M. Sofin, M. Jansen, and B. Keimer, Phys. Rev. Lett. **101**, 047202 (2008).
[22] J. Málek, S.-L. Drechsler, S. Flach, E. Jeckelmann, and K. Kladko, J. Phys. Soc. Jpn. **72**, 2277 (2003).
[23] M. Matsuda, K. Kakurai, S. Kurogi, K. Kudo, Y. Koike, H. Yamaguchi, T. Ito, and K. Oka, Phys. Rev. B **71**, 104414 (2005).
[24] M. Isobe, M. Onoda, T. Ohta, F. Izumi, K. Kimoto, E. Takayama-Muromachi, A. W. Hewat, and K. Ohoyama, Phys. Rev. B **62**, 11667 (2000).
[25] E. Müller-Hartmann, J. Low Temp. Phys. **99**, 349 (1995), often the zigzag chain is considered which is topologically equivalent to the Hubbard chain with first-neighbor and second-neighbor hopping.
[26] K. Penc, H. Shiba, F. Mila, and T. Tsukagoshi, Phys. Rev. B **54**, 4056 (1996).
[27] P. Pieri, S. Daul, D. Baeriswyl, M. Dzierzawa, and P. Fazekas, Phys. Rev. B **54**, 9250 (1996).
[28] S. Daul and R. M. Noack, Phys. Rev. B **58**, 2635 (1998).
[29] S. Nishimoto, K. Sano, and Y. Ohta, Phys. Rev. B **77**, 085119 (2008).
[30] E. Lieb and D. Mattis, Phys. Rev. **125**, 164 (1962).
[31] J. Schnack and F. Ouchni, J. Magn. Magn. Mater. **290**, 341 (2005).
[32] R. Klingeler, B. Büchner, K.-Y. Choi, V. Kataev, U. Ammerahl, A. Revcolevschi, and J. Schnack, Phys. Rev. B **73**, 014426 (2006).
[33] Y. Mizuno, T. Tohyama, S. Maekawa, T. Osafune, N. Motoyama, H. Eisaki, and S. Uchida, Phys. Rev. B **57**, 5326 (1998).
[34] S. Tornow, O. Entin-Wohlman, and A. Aharony, Phys. Rev. B **60**, 10206 (1999).
[35] T. Masuda, A. Zheludev, A. Bush, M. Markina, and A. Vasiliev, Phys. Rev. Lett. **92**, 177201 (2004).
[36] L. Capogna, M. Mayr, P. Horsch, M. Raichle, R. K. Kremer, M. Sofin, A. Maljuk, M. Jansen, and B. Keimer, Phys. Rev. B **71**, 140402(R) (2005).
[37] S.-L. Drechsler, J. Richter, A. A. Gippius, A. Vasiliev, A. A. Bush, A. S. Moskvin, J. Málek, Y. Prots, W. Schnelle, and H. Rosner, Europhys. Lett. **73**, 83 (2006).
[38] S.-L. Drechsler, O. Volkova, A. N. Vasiliev, N. Tristan, J. Richter, M. Schmitt, H. Rosner, J. Málek, R. Klingeler, A. A. Zvyagin, and B. Büchner, Phys. Rev. Lett. **98**, 077202 (2007).
[39] D. J. Thouless, Proc. Phys. Soc. Jpn. **86**, 893 (1965).
[40] A. D. Klironomos, J. S. Meyer, T. Hikihara, and K. A. Matveev, Phys. Rev. B **76**, 075302 (2007).
[41] B. Valenzuela, S. Fratini, and D. Baeriswyl, Phys. Rev. B **68**, 045112 (2003).
[42] M. Mayr and P. Horsch, Phys. Rev. B **73**, 195103 (2006).
[43] A typical size of t_1 is 50 meV in edge-sharing chains as compared to 500 meV in 180° bonds as in the high-T_c or ladder compounds.
[44] M. Daghofer and P. Horsch, Phys. Rev. B **75**, 125116 (2007).
[45] R. Arita, Y. Shimoi, K. Kuroki, and H. Aoki, Phys. Rev. B **57**, 10609 (1998).
[46] S. Daul and R. Noack, Z. Phys. B: Condens. Matter **103**, 293 (1997).
[47] R. Jackiw and C. Rebbi, Phys. Rev. D **13**, 3398 (1976).
[48] M. J. Rice and E. J. Mele, Phys. Rev. B **25**, 1339 (1982).
[49] S. Fratini and G. Rastelli, Phys. Rev. B **75**, 195103 (2007).
[50] F. Pollmann, P. Fulde, and K. Shtengel, Phys. Rev. Lett. **100**, 136404 (2008).